



SYNTHESIS, DFT ANALYSIS, ANTIMICROBIAL ACTIVITY AND DOCKING INTERACTIONS OF SOME POTENTIAL PYRAZOLE AND 1,3,4-OXADIAZOLES MOTIFS DERIVED FROM 2-(4-(3-NITROIMIDAZO[1,2-*b*]PYRIDAZIN-6-YL) PIPERAZIN-1-YL) ACETOHYDRAZIDE

B. Subba Rao¹, P. Sanjeeva¹, S. Akkulanna² and P. Venkata Ramana^{1*}

¹*Department of Chemistry, Sri Krishnadevaraya University, Ananthapuramu-515003, Andhra Pradesh, India.*

²*Department of Botany, Sri Krishnadevaraya University, Ananthapuramu-515003, Andhra Pradesh, India.*

**Corresponding author E-Mail: ramanapv54@gmail.com*

ABSTRACT:

The development of new antimicrobial drugs is most needed due to rapid growth in global antimicrobial resistance. In this connection, a series of novel substituted pyrazoles & 1,3,4-oxadiazole derivatives (4a-f and 7a-f) were synthesized. Further DFT calculation was carried out at B3LYP/lanL2dZ level of theory. *In-silico* studies were carried with Auto Dock 4.2/ADT program. The studies revealed that all the compounds have shown significant binding affinity with BAX protein. All the derivatives were evaluated for their *in-vitro* antibacterial, antifungal activity against Gram-positive (*Bacillus cereus*), Gram-negative (*Escherichia coli*) bacteria and fungi (*Candida albicans*). The culture plates were examined to measure the zone of inhibition at optimal concentration. Majority of the derivatives have shown significant biological activity with potency comparable to standard drugs Amoxicillin and Amphotericin-B.

KEY WORDS: DFT, Molecular docking, Acetohydrazides, Pyrazoles, 1,3,4-oxadiazoles, Antibacterial activity, antifungal activity.

INTRODUCTION:

Antibiotic resistance emerges in bacteria and other hazardous microbes through a variety of adaptations and pathwaysⁱ. Anti-microbial resistance (AMR), developing resistance to the existing antibiotics and therapies by pathogenic bacteria and other microbes, is the global health concern^{ii,iii}. Drug-resistant microbial infections are difficult to treat and have an impact on the world economy, particularly in developing and low-income nations. The lack of effective antibacterial agents, as well as the growing AMR among other harmful bacteria and microorganisms, has caught the attention of the international scientific community and the pharmaceutical business^{iv, v}. The understanding of the likely causes and mechanisms underlying the rise in AMR, as well as the prevention and treatment of infections with drug

resistance, have undergone major improvements in recent years. AMR was successfully combated by creating powerful chemicals and antibiotics, primarily using new heterocyclic compounds^{vi-xi}. Heterocyclic compounds are a rich supply of functional active molecules with a variety of biological roles, including those of oxygen carriers (hemoglobin), energy stores (adenosine triphosphate), genetic materials (DNA), neurotransmitters, and naturally occurring antibacterial agents (diketopiperazines)^{xii}. Heterocyclic compounds with various functional moieties have been investigated for their antibacterial effects because of the various biological activities. Pyrazoles, 1,3,4-oxadiazoles, and molecules with nitrogen-rich five-membered heterocyclic structures are the essential source of physiologically active chemicals for a variety of uses^{xiii-xx}. Pyrazoles and 1,2-diazoles are five-membered heterocyclic compounds with two nitrogens in the structure. The development and investigation of compounds with pyrazole moieties for their anti-inflammatory, anti-convulsant, anti-cancer, ACE inhibitor, anti-viral, and anti-microbial research has been fruitful^{xxi-xxvi}. In addition to the naturally occurring pyrazole nuclei found in a small number of physiologically useful substances created synthetically, these nuclei have a variety of features, including anti-diabetic and anti-cancer effects^{xxvii}. Medicine-active natural substances with pyrazole-moiety incorporated into the integral structure include Pyrazole-3 (5)-carboxylic acid, Fluviois A-E, Pyrazofurin, and Formycin. Examples of medications with an embedded pyrazole moiety in their structure include amino phenazone, phenazone, sulfinpyrazone, and phenylbutazone. Oxadiazoles are five-membered heterocyclic compounds that contain two nitrogen atoms and one oxygen. Widely available natural compounds with a variety of medicinal characteristics include oxadiazole scaffolds. 1,3,4-Oxadiazole derivatives, which are oxadiazole-containing substances, are widely known for their anti-inflammatory, analgesic, agonistic fatty acid receptor, anti-tumor, and antibacterial effects^{xxviii, xxix}. Pyrazole and oxadiazole derivatives are clearly medicinally significant molecules with a variety of biological activities, including antibacterial capabilities, as evidenced by their existence in natural products and recent discoveries^{xxx-xxxiv}. The combination of both active moieties would, as we had predicted i.e., pyrazoles and oxadiazoles with appropriate chemistry would result in novel and potent class of antibacterial compounds. However, there are barely any systematic studies reporting development and antibacterial activities of such substituted pyrazole/ 1,3,4-oxadiazole compounds. Hybrids of 1,3,4-oxadiazole have recently been effectively produced to treat various tumors and infectious illness^{xxxv}. In this attempt, we have prepared a library of rationally designed and selectively substituted pyrazole/ 1,3,4-oxadiazole derivatives (4a-f and 7a-f). The synthesized compounds were screened for superior antibacterial activity against one Gram-positive, one Gram-negative bacteria and antifungal activity against one fungus. DFT and Molecular docking studies were also performed to accurately predict molecular structure, properties and study the binding interaction modes of synthesized compounds with the active site of the BAX protein. The results of *in vitro* and docking studies showed that substituted pyrazole/1,3,4-oxadiazole derivatives may serve as new antibacterial agents.

EXPERIMENTAL:

All the reagents and commercial solvents were used without further purification. Melting points were determined by using a Buchi 535 melting point apparatus and were uncorrected. The visualization of compounds was performed with UV light at 254 and 365 nm, I₂ and heating plates dipping in 2% phosphomolybdic acid in 15% aq. H₂SO₄ solution. The reactions were monitored by thin layer chromatography carried on precoated silica gel 60F254 plates (Merck). ¹³C NMR spectra using CDCl₃ as internal standard were recorded on a Varian Unity 100 MHz NMR spectra using TMS as an internal standard were recorded on a

BRUKER 400 MHz and Mass spectra were performed on a VG Micro mass 7070H and a Finnigan Mat 1020B mass spectrometer at 70 eV.

Computational Methods

The Gaussian-09 program was used to carry out the DFT computations^{xxxvi}. And Gauss view 5 for visualizing molecule structures and attributes resulting from Gaussian calculations, to visualize the data.

Molecular Docking

The optimized structures of the BAX, hydrazones and 1,3,4-oxadiazole derivatives were used for molecular docking calculations. Molecular docking was carried out with the automated docking program, Auto Dock 4.2^{xxxvii-xxix}. All the components such as BAX, hydrazones and 1,3,4-oxadiazole derivatives were optimized before conducting docking and the results were analyzed using binding energy. For each ligand, a docking experiment consisting of 100 simulations was performed and the analysis was based on binding-free energies and root-mean-square deviation (RMSD) values. Docking with all the newly synthesized compounds was performed onto BAX with the same parameters and PMV 1.4.5 viewer was then used to observe the interactions of the docked compound to the BAX protein, further docking analysis was carried out on PyMol software.

Antimicrobial Activity

The antibacterial and antifungal activities of the synthesized compounds were examined by disc diffusion method against the bacterial strains: *Escherichia coli*, *Bacillus cereus* and fungus *Candida albicans* as compared to the standard drug Amoxycillin and Amphotericin-B respectively.

The antimicrobial activities were evaluated by disc diffusion method with nutrient agar medium (NAM) for bacterial and potato dextrose agar (PDA) medium for fungal culture respectively. Both the media were sterilized in an autoclave at 121°C, 15 lbs. pressure for 30 minutes. After sterilization approximately 20 ml of molten and cooled media was poured in sterilized Petri dishes. The plates were leftover for 30 min. The test compounds were dissolved in DMSO at a concentration of 400 µg/ml. The stock solutions were applied to each sterilized filter paper disc of 5 mm. Discs were dried and preserved for antimicrobial study. The discs were placed on NAM and PDA inoculated with bacteria or fungi and NAM plates were incubated at 37°C and PDA plates at 30°C for 24-30 hrs. The plates were examined to measure the zone of inhibition at 400 µg/mL concentration. The mean values of the radius of zone of inhibition were measured by repeating the experiments thrice.

GENERAL PROCEDURE:

Synthesis of Ethyl 2-(4-(3-nitroimidazo[1,2-*b*] pyridazin-6-yl) piperazin-1-yl) acetate (1)
3-Nitro-6-(piperazin-1-yl) imidazo[1,2-*b*] pyridazine was dissolved in Dry DMF (10 volumes) and cooled to 0°C in ice cold water. Ethyl bromo acetate 1.1 Eq was added drop wise and kept at room temperature for 16 hrs.

TLC confirmed the completion of the reaction and reaction mass was poured into saturated ammonium chloride solution. The product was extracted with ethyl acetate (twice). The organic layer was dried over anhydrous sodium sulphate and evaporated to afford the crude product. The crude product was purified by silica gel column chromatography eluted with 2% methanol in chloroform to afford the product as light-yellow solid (82%).

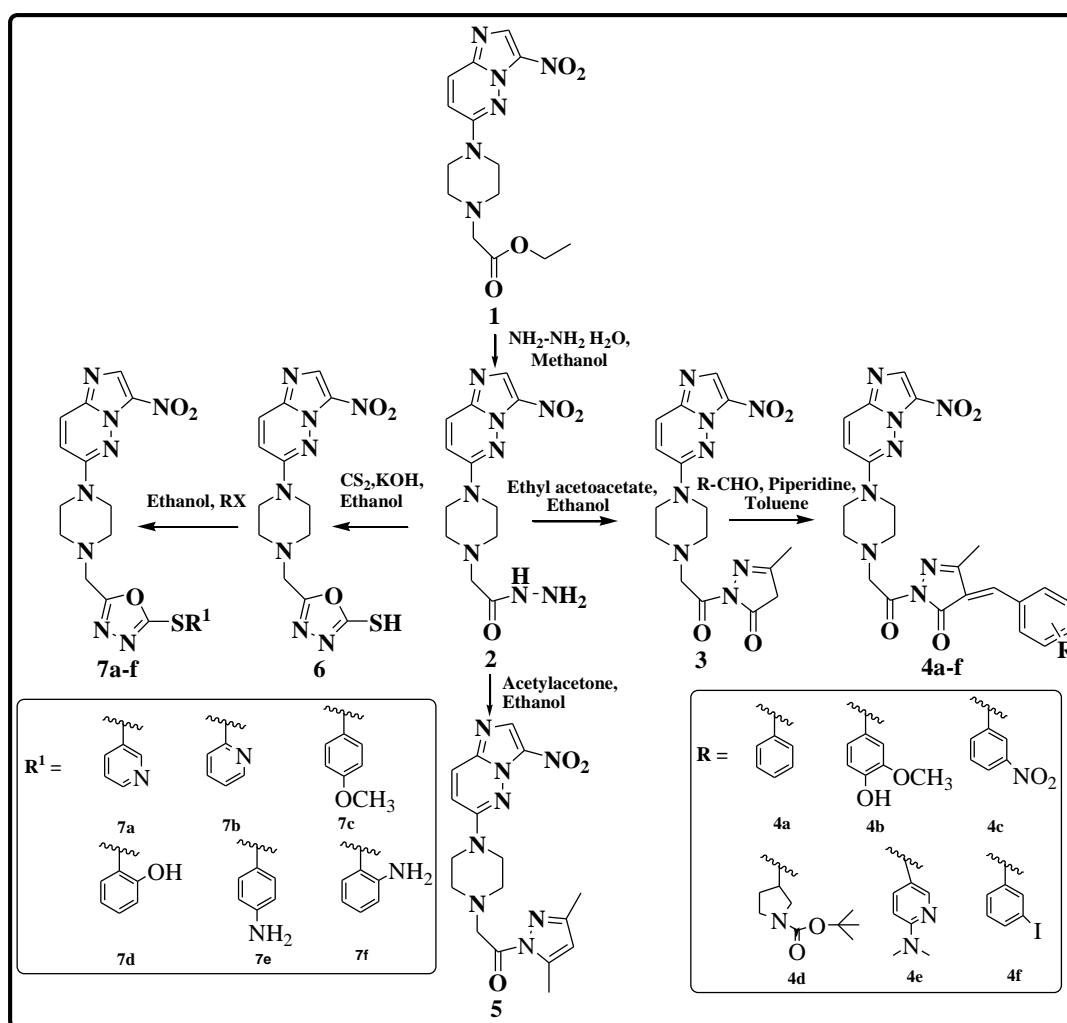
Synthesis of 2-(4-(3-nitroimidazo[1,2-*b*] pyridazin-6-yl) piperazin-1-yl)Aceto hydrazide (2)

Ethyl 2-(4-(3-nitroimidazo[1,2-*b*] pyridazin-6-yl) piperazin-1-yl) acetate (1) (1 Eq) was dissolved in ethanol (15 volumes). 3 Eq of hydrazine hydrate was added and the reaction mass was heated at reflux for 6 hrs. Reaction completion was confirmed by TLC and

evaporated to crude. The crude product was suspended in ethyl acetate, washed with water and brine. The organic layer was dried over sodium sulphate and evaporated to afford the pure product as off-white solid, which was directly used for the next step without further purifications (76%).

Synthesis of 3-methyl-1-(2-(4-(3-nitroimidazo[1,2-*b*]pyridazin-6-yl)piperazin-1-yl)acetyl)-1*H*-pyrazol-5(4*H*)-one (3)

A mixture of ethyl acetoacetate (0.01 mol) and 2-(4-(3-nitroimidazo[1,2-*b*]pyridazin-6-yl)piperazin-1-yl)acetohydrazide (2) (0.02 mol) in ethanol (20 mL) was heated under reflux for 10 hrs. on a water bath. After completion of the reaction, ethanol evaporated. The residue was treated with water, neutralized with NaHCO₃ and extracted with ether. Then the ether solution was evaporated under reduced pressure to furnish the pure compound. It was recrystallized from ethanol.



Scheme: Synthesis of 4-(substituted benzylidene)-3-methyl-1-(2-(4-(3-nitroimidazo[1,2-*b*]pyridazin-6-yl)piperazin-1-yl)acetyl)-1*H*-pyrazol-5(4*H*)-ones (4a-f), 1-(3,5-dimethyl-1*H*-pyrazol-1-yl)-2-(4-(3-nitroimidazo[1,2-*b*]pyridazin-6-yl)piperazin-1-yl)ethanone (5) and 3-nitro-6-(4-((5-(substituted-ylthio)-1,3,4-oxadiazol-2-yl)methyl)piperazin-yl)imidazo[1,2-*b*]pyridazines (7a-f).

Synthesis of 4-benzylidene-3-methyl-1-(2-(4-(3-nitroimidazo[1,2-*b*]pyridazin-6-yl)piperazin-1-yl)acetyl)-1*H*-pyrazol-5(4*H*)-one (4a)

3-Methyl-1-(2-(4-(3-nitroimidazo[1,2-*b*]pyridazin-6-yl)piperazin-1-yl)acetyl)-1*H*-pyrazol-5(4*H*)-one (3) (0.01 mol) and benzaldehyde (0.01 mol) suspended in dry toluene were taken in a flask equipped with a Dean-Stark apparatus fitted with a calcium chloride guard tube. Then catalytic amount of piperidine (0.5 mL) was added and the reaction mixture was refluxed with stirring for about 8 hrs. The progress of the reaction was monitored by TLC until the disappearance of starting materials. The product precipitated on cooling was washed with methanol and purified by recrystallization from a mixture of ethanol and chloroform (1:1).

Compounds **4b-f** were prepared similarly, taking appropriate substituted aldehyde in place of benzaldehyde.

Synthesis of 1-(3,5-dimethyl-1*H*-pyrazol-1-yl)-2-(4-(3-nitroimidazo[1,2-*b*]pyridazin-6-yl)piperazin-1-yl)ethanone (5)

A mixture of acetylacetone (0.01 mol) and 2-(4-(3-nitroimidazo[1,2-*b*]pyridazin-6-yl)piperazin-1-yl)acetohydrazide (2) (0.02 mol) in ethanol (20 mL) was heated under reflux for 8 hrs. on a water bath. After completion of the reaction, ethanol was evaporated, the residue was dissolved in water, neutralized with NaHCO₃ and extracted with ether. The ether solution was evaporated under reduced pressure to furnish the pure compound. The product was recrystallized from ethanol.

Synthesis of 5-((4-(3-nitroimidazo[1,2-*b*]pyridazin-6-yl)piperazin-1-yl)methyl)-1,3,4-oxadiazole-2-thiol (6)

2-(4-(3-Nitroimidazo[1,2-*b*]pyridazin-6-yl)piperazin-1-yl)acetohydrazide (2) (0.01 mol), KOH 0.01 mol (0.56 g) and 10 mL of carbon disulphide were together refluxed in 50 mL of 95% ethanol for 10 hrs. The resultant mixture was concentrated and cooled to room temperature. The product obtained was acidified with dil. HCl. The solid mass separated out was filtered, dried and purified by recrystallization from ethanol.

Synthesis of 3-nitro-6-(4-((5-(pyridin-3-ylthio)-1,3,4-oxadiazol-2-yl)methyl)piperazin-1-yl)imidazo[1,2-*b*]pyridazine (7a)

5-((4-(3-Nitroimidazo[1,2-*b*]pyridazin-6-yl)piperazin-1-yl)methyl)-1,3,4-oxadiazole-2-thiol (3) and 3-chloropyridine in equimolar quantities were refluxed in 95% ethanol for 2 hrs. The reaction mixture was monitored by TLC until the disappearance of starting materials. The resultant solution was concentrated under reduced pressure. The product was dissolved in ethyl acetate and the organic phase was successively washed with 5% HCl, 5% Na₂CO₃ solution, water (2 x 40 mL) and the organic layer was collected, washed with brine solution, dried over anhydrous Na₂SO₄ and ethyl acetate decanted off. The ethyl acetate was then concentrated under reduced pressure. The solid mass separated out was collected, dried and recrystallized from ethanol to obtain **7a**. Compounds **7b-f** were similarly obtained, substituting 2-chloropyridine with different chloro-compounds.

RESULTS AND DISCUSSION:

The details with regard to the synthesis and characterization of Ethyl 2-(4-(3-nitroimidazo[1,2-*b*]pyridazin-6-yl)piperazin-1-yl)acetate(1), and 2-(4-(3-nitroimidazo[1,2-*b*]pyridazin-6-yl)piperazin-1-yl)acetohydrazide (2) has been discussed in our research article

A mixture of ethyl acetoacetate and 2-(4-(3-nitroimidazo[1,2-*b*]pyridazin-6-yl)piperazin-1-yl)acetohydrazide 2 in ethanol (20 mL) was heated under reflux for 10 hrs. on a water bath. After completion of the reaction, ethanol evaporated. The residue was treated with water, neutralized with NaHCO₃ and extracted with ether. Ether layer was then evaporated under

reduced pressure to furnish the pure compound 3. It was recrystallized from ethanol. The ^1H NMR spectrum of compound 3 displayed signals at δ 2.326 and 3.184 ppm for methyl and methylene protons of the pyrazoline ring respectively. The ^{13}C NMR spectrum of compound 3 displayed signals at δ 24.35 and 44.64 ppm for the methyl and methylene carbon atoms of the pyrazoline ring respectively that confirm the structure of compound 3.

Formation of 5-((4-(3-nitroimidazo[1,2-*b*]pyridazin-6-yl)piperazin-1-yl)methyl)-1,3,4-oxadiazole-2-thiol 6 has been confirmed by ^1H NMR, ^{13}C NMR and Mass spectral analysis. In proton NMR a broad signal for SH proton of thiol appears at δ 3.547-3.848 ppm merged with the signal of piperazine ring confirms the formation of compound 6. The signal for two protons of the pyridazine ring appears as a multiplet at 8.118-8.156 ppm. The signal for imidazole proton appears as a singlet at δ 8.345 ppm. In mass spectrum a peak appears at m/z 362.02 corresponding to $[\text{M}+\text{H}]$ ion of compound 6. The ^{13}C NMR spectral data has been found consistent with the structure of compound 6.

3-Methyl-1-(2-(4-(3-nitroimidazo[1,2-*b*]pyridazin-6-yl)piperazin-1-yl)acetyl)-1*H*-pyrazol-5(4*H*)-one (3)

Light Yellow solid; Yield: 96.0%, m.p: 126-128°C

^1H NMR (400 MHz, DMSO- d_6): δ 1.326 (s, 3H, CH₃), 2.699-2.799 (t, 4H, J = 5.0 Hz, piperazine ring), 3.184 (s, 2H, CH₂), 3.688-3.708 (t, 4H, J = 5.1Hz, piperazine ring), 3.905 (s, 2H, CH₂), 7.088-7.108 (d, 1H, J = 8 Hz, pyridazine ring), 7.846-7.866 (d, 1H, J = 8 Hz, pyridazine ring), 8.403 (s, 1H, imidazole ring).

^{13}C NMR (100 MHz, DMSO- d_6): δ 24.35, 44.64, 50.01, 52.56, 56.48, 116.45, 125.87, 130.78, 138.62, 145.23, 156.86, 160.32, 162.85, 171.02.

MS m/z : 387.15 $[\text{M}+\text{H}]$, (386.15); Anal. Calcd. (found) % for C₁₆H₁₈N₈O₄: C, 49.74(49.57); H, 4.70(4.52); N, 29.00(28.86).

4-benzylidene-3-methyl-1-(2-(4-(3-nitroimidazo[1,2-*b*]pyridazin-6-yl)piperazin-1-yl)acetyl)-1*H*-pyrazol-5(4*H*)-one (4a)

Yellow solid; Yield: 84.0%, m.p: 132-134°C

^1H NMR (400 MHz, DMSO- d_6): δ 0.941 (s, 3H, CH₃), 3.300 (s, 4H, piperazine ring), 3.713 (s, 4H, piperazine ring), 6.721-6.742 (d, 1H, J = 8.4 Hz, pyridazine ring), 6.817-6.837 (d, 1H, J = 8.4 Hz, pyridazine ring), 6.954 (s, 1H, =CH), 7.312-7.495 (m, 6H, phenyl ring and imidazole ring),

^{13}C NMR (100 MHz, DMSO- d_6): δ 29.74, 45.71, 55.62, 55.85, 112.02, 115.83, 121.00, 123.48, 126.28, 127.22, 127.26, 128.87, 129.54, 140.48, 141.27, 143.63, 147.75, 148.59, 156.01, 165.25, 170.75.

MS m/z : 475.18 $[\text{M}+\text{H}]$, (474.18); Anal. Calcd. (found) % for C₂₃H₂₂N₈O₄: C, 58.22(58.02); H, 4.67(4.38); N, 23.62(23.45).

4-(4-hydroxy-3-methoxybenzylidene)-3-methyl-1-(2-(4-(3-nitroimidazo[1,2-*b*]pyridazin-6-yl)piperazin-1-yl)acetyl)-1*H*-pyrazol-5(4*H*)-one (4b)

Color less solid; Yield: 74.0%, m.p: 138-140°C

^1H NMR (400 MHz, DMSO- d_6): δ 1.228 (s, 3H, CH₃), 2.668-2.778 (m, 4H, piperazine ring), 3.164 (s, 2H, CH₂), 3.652-3.693 (m, 4H, piperazine ring), 3.819 (s, 3H, OCH₃), 4.055 (s, 1H, OH), 6.804-6.839 (m, 1H, phenyl ring), 7.041-7.061 (m, 1H, phenyl ring), 7.041-7.061 (m, 1H, phenyl ring), 7.580,7.605 (d, 1H, J =10.0Hz, pyridazine ring), 8.103-8.200 (m, 1H, pyridazine ring), 8.526 (s, 1H, imidazole ring), 9.485-9.542 (doublet like, 1H, =CH).

^{13}C NMR (100 MHz, DMSO- d_6): δ 25.54, 45.25, 51.85, 55.55, 60.19, 114.91, 115.40, 115.56, 120.91, 122.04, 125.62, 126.69, 134.92, 143.32, 147.77, 147.89, 148.00, 148.60, 148.92, 155.71, 165.07, 170.47.

MS m/z: 521.18 [M+H], (520.18); Anal. Calcd. (found) % for C₂₄H₂₄N₈O₆: C, 55.38(55.18); H, 4.65(4.47); N, 21.53(21.36).

4-(3-nitrobenzylidene)-3-methyl-1-(2-(4-(3-nitroimidazo[1,2-*b*]pyridazin-6-yl)piperazin-1-yl)acetyl)-1*H*-pyrazol-5(4*H*)-one (4c)

White solid; Yield: 78.0%, m.p: 145-147°C

¹H NMR (400 MHz, DMSO-*d*₆): δ 1.227 (s, 3H, CH₃), 2.738 (s, 2H, CH₂), 3.364 (s, 4H, piperazine ring), 3.720 (s, 4H, piperazine ring), 7.592-7.634 (s, 1H, pyridazine ring), 7.727-7.756 (m, 1H, phenyl ring), 8.109-8.263 (m, 4H, pyridazine ring, =CH, phenyl ring), 8.463-8.549 (m, 2H, imidazole ring, phenyl ring).

¹³C NMR (100 MHz, DMSO-*d*₆): δ 27.64, 44.87, 51.61, 52.02, 114.94, 120.90, 124.23, 126.73, 126.87, 130.47, 133.01, 133.87, 134.94, 135.77, 136.13, 138.23, 144.86, 148.23, 155.67, 164.25, 171.89.

MS m/z: 520.16 [M+H], (519.16); Anal. Calcd. (found) % for C₂₃H₂₁N₉O₆: C, 53.18(52.95); H, 4.07(3.88); N, 24.27(24.08).

tert-butyl 3-(3-methyl-1-(2-(4-(3-nitroimidazo[1,2-*b*]pyridazin-6-yl)piperazin-1-yl)acetyl)-5-oxo-1*H*-pyrazol-4(5*H*)-ylidene)methyl)pyrrolidine-1-carboxylate (4d)

Dull white solid; Yield: 78.0%, m.p: 165-167°C

¹H NMR (400 MHz, DMSO-*d*₆): δ 1.278 (s, 3H, CH₃), 2.509-2.768 (m, 10H, piperazine and pyrrolidine ring), 2.894 (s, 1H, CH), 3.071-3.083 (d, 9H, *J*= 4.8 Hz, (CH₃)₃), 3.373 (s, 2H, CH₂), 3.642-3.692 (m, 4H, piperazine ring), 6.687-6.783 (d, 1H, *J*= 11.2 Hz, pyridazine ring), 7.580-7.606 (d, 1H, *J*= 10.4 Hz, pyridazine ring), 8.115 (s, 1H, imidazole ring), 8.572 (s, 1H, =CH).

¹³C NMR (100 MHz, DMSO-*d*₆): δ 28.54, 30.02, 30.16, 32.10, 35.81, 37.62, 45.06, 51.95, 56.97, 60.21, 114.19, 117.96, 126.71, 134.01, 138.24, 145.86, 148.76, 155.73, 159.45, 164.95, 170.14.

MS m/z: 568.26 [M+H], (567.26); Anal. Calcd. (found) % for C₂₆H₃₃N₉O₆: C, 55.02(54.89); H, 5.86(5.68); N, 22.21(22.08).

4-((6-(Dimethylamino)pyridin-3-yl)methylene)-3-methyl-1-(2-(4-(3-nitroimidazo[1,2-*b*]pyridazin-6-yl)piperazin-1-yl)acetyl)-1*H*-pyrazol-5(4*H*)-one (4e)

White solid; Yield: 78.0%, m.p: 155-157°C

¹H NMR (400 MHz, DMSO-*d*₆): δ 1.233 (s, 3H, CH₃), 1.382-1.416 (m, 6H, -N(CH₃)₂), 2.675-2.894 (m, 4H, piperazine ring), 3.660 (s, 6H, piperazine ring and CH₂), 7.035-7.067 (m, 2H, pyridine ring), 7.576-7.601 (d, 1H, *J*= 10 Hz, pyridazine ring), 8.118-8.143 (d, 1H, *J*=10 Hz, pyridazine ring), 8.531 (s, 1H, imidazole ring), 8.811-8.841 (m, 2H, pyridine ring and =CH).

¹³C NMR (100 MHz, DMSO-*d*₆): δ 28.21, 44.89, 51.32, 58.16, 65.38, 114.99, 123.65, 123.76, 132.13, 134.99, 138.27, 140.12, 145.56, 153.95, 156.41, 161.20, 163.14, 165.52, 169.24, 171.03.

MS m/z: 519.21 [M+H], (518.21); Anal. Calcd. (found) % for C₂₄H₂₆N₁₀O₄: C, 55.59(55.40); H, 5.05(4.93); N, 27.01(26.85).

4-(3-iodobenzylidene)-3-methyl-1-(2-(4-(3-nitroimidazo[1,2-*b*]pyridazin-6-yl) piperazin-1-yl)acetyl)-1*H*-pyrazol-5(4*H*)-one (4f)

Yellow solid; Yield: 70.0%, m.p: 144-146°C

¹H NMR (400 MHz, DMSO-*d*₆): δ 1.255 (s, 3H, CH₃), 2.801, 2.811, 2.820, (t, 4H, *J*= 4.9 Hz, piperazine ring), 3.339 (s, 2H, CH₂), 3.374, 3.774, 3.784 (t, 4H, *J*= 4.9 Hz, piperazine ring), 7.114-7.134 (d, 1H, *J*= 10 Hz, pyridazine ring), 7.512-7.534 (dd, 1H, *J*₁= 8.8 Hz, *J*₂= 2.2 Hz, pheny ring), 7.873-7.893 (d, 1H, *J*= 10 Hz, pyridazine ring), 8.020-8.053 (m, 2H, phenyl ring), 8.277-8.282 (d, 1H, *J*= 2.2 Hz, phenyl ring), 8.418 (s, 1H, =CH), 8.793 (s, 1H, imidazole ring).

¹³C NMR (100 MHz, DMSO-*d*₆): δ 24.05, 50.23, 52.55, 56.42, 104.56, 118.47, 125.33, 125.65, 126.78, 128.15, 130.92, 133.54, 136.41, 137.95, 138.52, 143.26, 145.87, 147.13, 156.32, 166.05, 171.10.

MS m/z: 601.07 [M+H], (600.07); Anal. Calcd. (found) % for C₂₃H₂₁N₈O₄: C, 46.01(45.92); H, 3.53(3.36); N, 18.66(18.45).

1-(3,5-Dimethyl-1*H*-pyrazol-1-yl)-2-(4-(3-nitroimidazo[1,2-*b*]pyridazin-6-yl)piperazin-1-yl)ethanone (5)

Yellow solid; Yield: 86.0%, m.p: 120-122°C

¹H NMR (400 MHz, DMSO-*d*₆): δ 1.324 (s, 3H, pyrazole CH₃), 2.700-2.800 (t, 4H, *J*= 5.0 Hz, piperazine ring), 3.186 (s, 3H, pyrazole CH₃), 3.690-3.710 (t, 4H, *J*= 5.1Hz, piperazine ring), 3.907 (s, 1H, pyrazole CH), 7.090-7.110 (d, 1H, *J*= 8 Hz, pyridazine ring), 7.848-7.868 (d, 1H, *J*= 8 Hz, pyridazine ring), 8.405 (s, 1H, imidazole ring).

¹³C NMR (100 MHz, DMSO-*d*₆): δ 17.35, 21.24, 50.01, 51.36, 52.42, 105.46, 122.37, 128.48, 135.64, 142.14, 146.23, 156.86, 158.21, 162.55, 181.02.

MS m/z: 385.17 [M+H], (384.17); Anal. Calcd. (found) % for C₁₇H₂₀N₈O₃: C, 53.28(53.12); H, 5.42(5.24); N, 29.38(29.15).

5-((4-(3-Ditroimidazo[1,2-*b*]pyridazin-6-yl)piperazin-1-yl)methyl)-1,3,4 oxadiazole-2-thiol (6)

Yellow solid; Yield: 76.0%, m.p: 168-170°C

¹H NMR (400 MHz, DMSO-*d*₆): δ 3.232 (s, 2H, CH₂), 3.547-3.848 (broad, 9H, piperazine ring and thiol), 8.118-8.156 (m, 2H, pyridazine ring), 8.345 (s, 1H, imidazole ring).

¹³C NMR (100 MHz, DMSO-*d*₆): δ 44.94, 52.08, 56.69, 114.91, 128.80, 129.88, 130.01, 133.85, 134.01, 134.25, 134.91.

MS m/z: 362.02 [M+H], (361.09); Anal. Calcd. (found) % for C₁₃H₁₄N₈O₃S: C, 43.09(42.85); H, 3.89(3.68); N, 30.92(30.64).

3-Nitro-6-(4-((5-(pyridin-3-ylthio)-1,3,4-oxadiazol-2-yl)methyl)piperazin-yl)imidazo[1,2-*b*]pyridazine (7a)

White solid; Yield: 68%, m.p: 152-154°C

¹H NMR (400 MHz, DMSO-*d*₆): δ 3.596-3.821 (broad signal, 6H, piperazine ring), 4.124-4.651 (broad signal, 2H, piperazine ring), 4.753 (s, 2H, CH₂), 7.674-7.699 (d, 1H, *J*= 10.0 Hz, pyridazine ring), 7.967-8.073 (m, 1H, pyridine ring), 8.253-8.286 (m, 1H, pyridazine ring), 8.607 (s, 1H, imidazole ring), 8.754-8.802 (m, 1H, pyridine ring), 8.923-8.935 (m, 1H, pyridine ring), 9.222 (s, 1H, pyridine ring).

¹³C NMR (100 MHz, DMSO-*d*₆): δ 42.47, 51.17, 55.64, 126.58, 127.38, 132.56, 134.09, 135.31, 138.55, 140.39, 140.51, 141.09, 142.91, 144.71, 155.36, 155.44.

MS m/z: 439.84 [M+H], (438.84); Anal. Calcd. (found) % for C₁₈H₁₇N₉O₃S: C, 49.20(48.90); H, 3.90(3.74); N, 28.69(28.42).

3-Nitro-6-(4-((5-(pyridin-2-ylthio)-1,3,4-oxadiazol-2-yl)methyl)piperazin-yl)imidazo[1,2-*b*]pyridazine (7b)

White solid; Yield: 73%, m.p: 162-164°C

¹H NMR (400 MHz, DMSO-*d*₆): δ 3.598-3.823 (broad signal, 6H, piperazine ring), 4.124-4.653 (broad signal, 2H, piperazine ring), 4.756 (s, 2H, CH₂), 6.926 (m, 2H pyridine ring), 7.426 (d, 1H, *J*= 6.8 Hz, pyridine ring), 7.676-7.701 (d, 1H, *J*= 10.0 Hz, pyridazine ring), 8.255-8.288 (m, 1H, pyridazine ring), 8.313 (d,1H, *J*= 7.2 Hz, pyridine ring), 8.609 (s, 1H, imidazole ring).

¹³C NMR (100 MHz, DMSO-*d*₆): δ 42.49, 51.15, 55.66, 126.60, 127.40, 132.58, 134.11, 135.31, 138.55, 140.40, 140.51, 141.09, 142.91, 144.73, 155.36, 155.46.

MS m/z: 439.84 [M+H], (438.84); Anal. Calcd. (found) % for C₁₈H₁₇N₉O₃S: C, 49.20(48.90); H, 3.90(3.74); N, 28.69(28.42).

6-(4-((5-(4-methoxyphenylthio)-1,3,4-oxadiazol-2-yl)methyl)piperazin-1-yl)-3-nitroimidazo[1,2-*b*]pyridazine (7c)

Light yellow solid; Yield: 73%, m.p: 160-162°C

¹H NMR (400 MHz, DMSO-*d*₆): δ 3.174 (s, 2H, CH₂), 3.590-3.693 (m, 8H, piperazine ring), 3.836 (s, 3H, OCH₃), 7.297-7.321 (m, 1H, pyridazine ring), 7.565-7.600 (dd, 2H, *J*= 4.0, 6.0, 4.0 Hz, phenyl ring), 7.942 (s, 1H, pyridazine ring), 8.096-8.133 (dd, 2H, *J*= 4.8, 5.2, 4.8 Hz, phenyl ring), 8.332 (s, 1H, imidazole ring).

¹³C NMR (100 MHz, DMSO-*d*₆): δ 45.02, 45.23, 51.79, 52.15, 57.06, 60.21, 114.89, 119.42, 119.49, 126.62, 126.68, 133.86, 134.91, 138.20, 142.04, 155.70, 165.19, 170.50.

MS *m/z*: 468.13 [M+H], (467.13); Anal. Calcd. (found) % for C₂₀H₂₀N₈O₄S: C, 51.27(51.04); H, 4.30(4.15); N, 23.92(23.72).

2-(5-((4-(3-Nitroimidazo[1,2-*b*]pyridazin-6-yl)piperazin-1-yl)methyl)-1,3,4-oxadiazol-2-ylthio)phenol (7d)

White solid; Yield: 73%, m.p: 160-161°C

¹H NMR (400 MHz, DMSO-*d*₆): δ 3.452-3.761 (m, 6H, piperazine ring), 4.250-4.443 (broad signal, 2H, piperazine ring), 4.694 (s, 2H, CH₂), 6.852-6.959 (m, 2H, phenyl ring), 7.257-7.275 (m, 1H, phenyl ring), 7.654-7.770 (m, 2H, pyridazine ring), 8.237-8.262 (m, 1H, phenyl ring), 8.428 (s, 1H, imidazole ring) 8.597 (s, 1H, OH).

¹³C NMR (100 MHz, DMSO-*d*₆): δ 42.65, 51.33, 51.50, 55.64, 55.90, 113.91, 116.44, 116.77, 119.63, 119.92, 127.40, 131.94, 134.21, 135.31, 138.63, 143.14, 155.51, 160.64, 165.94.

MS *m/z*: 455.12 [M+H], (454.12); Anal. Calcd. (found) % for C₁₉H₁₈N₈O₄S: C, 50.21(50.07); H, 3.99(3.78); N, 24.66(24.42).

4-(5-((4-(3-Nitroimidazo[1,2-*b*]pyridazin-6-yl)piperazin-1-yl)methyl)-1,3,4-oxadiazol-2-ylthio)benzenamine (7e)

Light Yellow solid; Yield: 75%, m.p: 165-168°C

¹H NMR (400 MHz, DMSO-*d*₆): δ 2.704 (s, 2H, CH₂), 3.240-3.525 (s, 6H, piperazine ring and NH₂), 3.706 (s, 4H, piperazine ring), 6.579-6.591 (d, 2H, *J* = 4.8 Hz, ArH), 6.950-6.962 (d, 2H, *J* = 4.8 Hz, ArH), 7.398-7.509 (m, 1H, pyridazine ring), 8.124-8.149 (m, 1H, pyridazine ring), 8.534 (singlet distorted, 1H, imidazole ring).

¹³C NMR (100 MHz, DMSO-*d*₆): δ 44.96, 51.70, 52.08, 114.96, 122.15, 122.19, 126.17, 128.85, 129.07, 133.89, 134.95, 136.76, 138.25, 145.41, 155.69.

MS *m/z*: 454.13 [M+H], (453.13); Anal. Calcd. (found) % for C₁₉H₁₉N₉O₃S: C, 50.32(50.20); H, 4.22(4.15); N, 27.80(27.64).

2-(5-((4-(3-Nitroimidazo[1,2-*b*]pyridazin-6-yl)piperazin-1-yl)methyl)-1,3,4-oxadiazol-2-ylthio)benzenamine (7f)

White solid; Yield: 78%, m.p: 164-166°C

¹H NMR (400 MHz, DMSO-*d*₆): δ 3.462 (s, 2H, ArNH₂), 3.570-3.989 (broad signal, 6H, piperazine ring), 4.426 (broad, 2H, piperazine ring), 4.705 (s, 2H, CH₂), 6.591-7.014 (m, 4H, ArH), 7.663-7.688 (d, 1H, *J*= 10 Hz, pyridazine ring), 8.262-8.287 (d, 1H, *J*= 10 Hz, pyridazine ring), 8.479 (s, 1H, imidazole ring).

¹³C NMR (100 MHz, DMSO-*d*₆): δ 42.40, 51.26, 55.58, 144.15, 127.04, 127.28, 127.56, 127.78, 130.07, 130.89, 133.48, 133.95, 135.26, 138.45, 141.70, 144.75, 166.38.

MS *m/z*: 454.13 [M+H], (453.13); Anal. Calcd. (found) % for C₁₉H₁₉N₉O₃S: C, 50.32(50.20); H, 4.22(4.15); N, 27.80(27.64).

Geometry optimization

The Gaussian-09 program was used to do geometry optimization for compounds 2, 4d, 4e, and 4f at the B3LYP/lanL2dZ level of theory. It has been shown that this computational

method accurately predicts molecule structure and related characteristics^{xli}. After the optimization, frequency analysis was carried out, which showed that there were no fictitious frequencies. This lack of fictitious frequencies demonstrates that the structures have undergone comprehensive optimization, guaranteeing their correctness and stability. Fig. 1 provides a visual representation of the optimized structures.

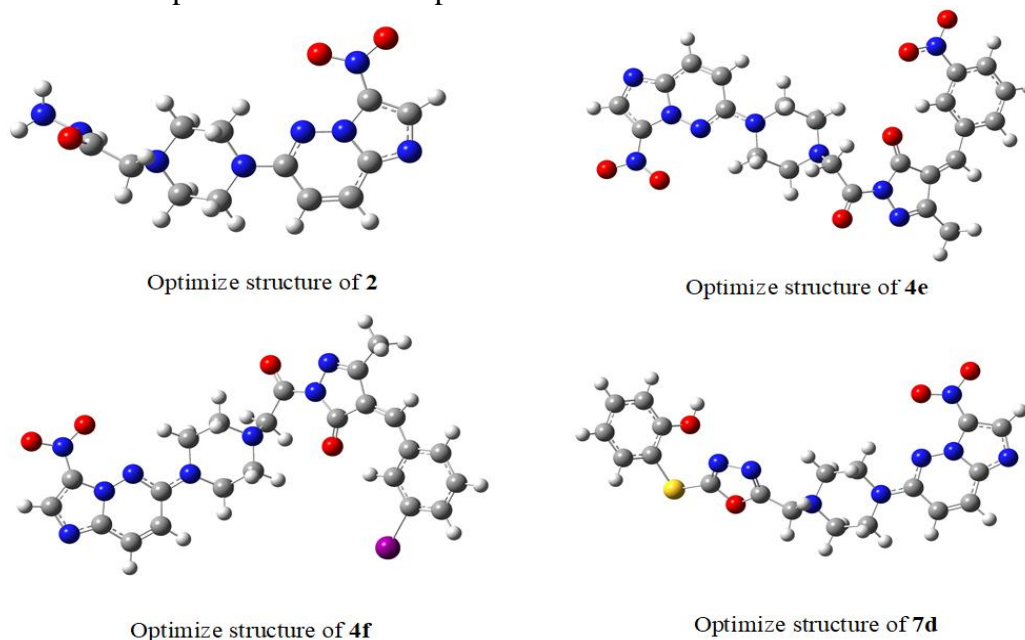


Fig. 1: Optimize structure of 2, 4e, 4f and 7d

MEP analysis

MEP (Molecular Electrostatic Potential) analysis was conducted for compounds 2, 4e, 4f, and 7d. MEP analysis is a valuable tool for studying hydrogen bonding and identifying reactive sites within molecules. In the MEP map, different colors correspond to various electrostatic potential values. Specifically, red indicates negative potential values, green represents zero potential, and blue signifies positive potential values. Fig. 2 shows MEP analysis of choosing compounds.

FMO Analysis

In this work, B3LYP/lanL2dZ level of theory was used to perform HOMO (Highest Occupied Molecular Orbital) and LUMO (Lowest Unoccupied Molecular Orbital) calculations for four different compounds, namely 2, 4d, 4e, and 4f. The findings are shown in Figure 3. A key method for understanding the electrical structure and chemical reactivity of molecules is the measurement of HOMO and LUMO energy levels^{xlii}. The HOMO specifically represents electron-donating capacity, whereas the LUMO represents electron-accepting capacity. The band gap values were calculated using the HOMO and LUMO data, and Table. 1 provides a summary of those results. A more band gap denotes more molecular stability, whereas a lower band gap denotes higher chemical reactivity.

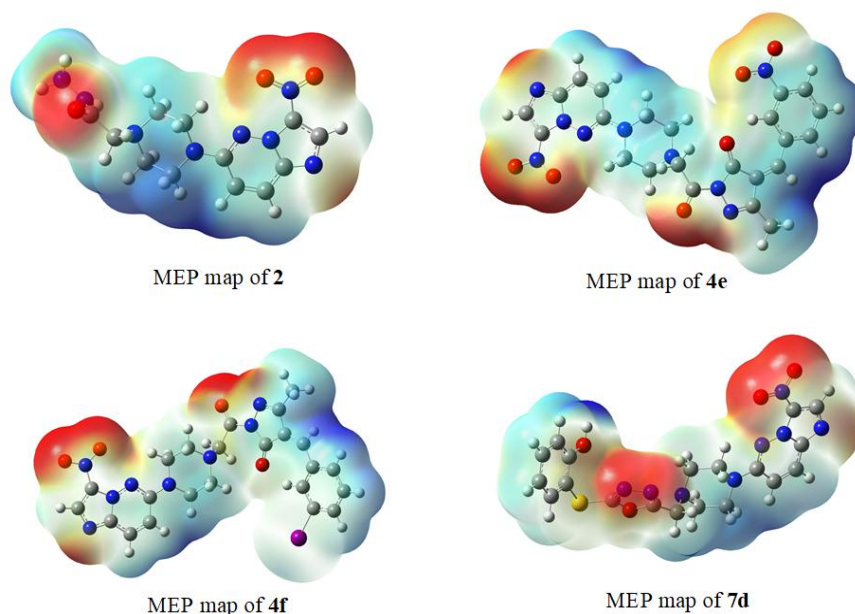


Fig. 2: MEP analysis of 2, 4e, 4f and 7d

It is estimated that compound 2 has the greatest band gap of the examined compounds, indicating more stability than the others. Compound 4e, on the other hand, has the lowest band gap, indicating a higher level of chemical reactivity. As a result, it is possible to determine that these compounds are reactive in the following order: $4e > 4f > 7d > 2$.

Additionally, several important reactivity descriptors were examined, such as ionization potential (I), electron affinity (A), chemical potential (μ), electronegativity (χ), hardness (η), softness (S), and electrophilicity index (ω). The HOMO-LUMO surfaces may be used to construct these global reactive descriptors, which are crucial in revealing important information about reactivity in the context of chemical processes. These descriptors are quantified using a variety of equations, which makes it easier to understand the reactivity profiles of the investigated substances.

$$\text{Ionization potential} = I = -E_{\text{HOMO}} \quad (1)$$

$$\text{Electron affinity} = A = -E_{\text{LUMO}} \quad (2)$$

$$\text{Electronegativity} = \chi = (I+A)/2 \quad (3)$$

$$\text{Chemical potential} = \mu = -\chi \quad (4)$$

$$\text{Hardness } \eta = (I-A)/2 \quad (5)$$

$$\text{Softness} = S = 1/\eta \quad (6)$$

$$\text{Electrophilicity index } \omega = \mu^2/2\eta \quad (7)$$

Table. 1 lists the global parameters determined for **2**, **4**, **4f** and **7d**. Band gap and chemical stability relate to hardness in a linear way. According to the hardness statistics, compound **2** is both harder and more stable than other compounds. Potential for chemical reactivity in softness. According to statistics on softness, compound **4e** is softer than other compounds and has a high chemical reactivity. All are electrophilic according to the electrophilicity index, although **4e** indicates higher electrophilic behavior. The order of electrophilicity is $4e > 4f > 2 > 7d$.

Table 1. Global parameters for 2, 4e, 4f and 7d.

	2	4e	4f	7d
HOMO	-6.2119 eV	-5.7972eV	-5.7435 eV	-5.9702 eV
LUMO	-3.0695 eV	-3.8123eV	-3.483 eV	-2.9533 eV
Band gap	3.1424 eV	1.9849 eV	2.26 eV	3.0169 eV
Ionization potential = $I = -E_{\text{HOMO}}$	6.2119 eV	5.7972 eV	5.7435 eV	5.9702 eV
Electron affinity = $A = -E_{\text{LUMO}}$	3.0695 eV	3.8123 eV	3.483 eV	2.9533 eV
Electronegativity = $\chi = (I+A)/2$	4.6407 eV	4.8047 eV	4.6132 eV	4.4618 eV
Chemical potential = $\mu = -\chi$	-4.6407 eV	-4.8047eV	-4.6132 eV	-4.4618 eV
Hardness $\eta = (I-A)/2$	1.5712 eV	0.9925 eV	1.1302 eV	1.5084 eV
Softness = $S = 1/\eta$	0.6364 eV	1.0075 eV	0.8848 eV	0.6629 eV
Electrophilicity index = $\omega = \mu^2/2\eta$	6.8534 eV	11.6298eV	9.415 eV	6.5019 eV

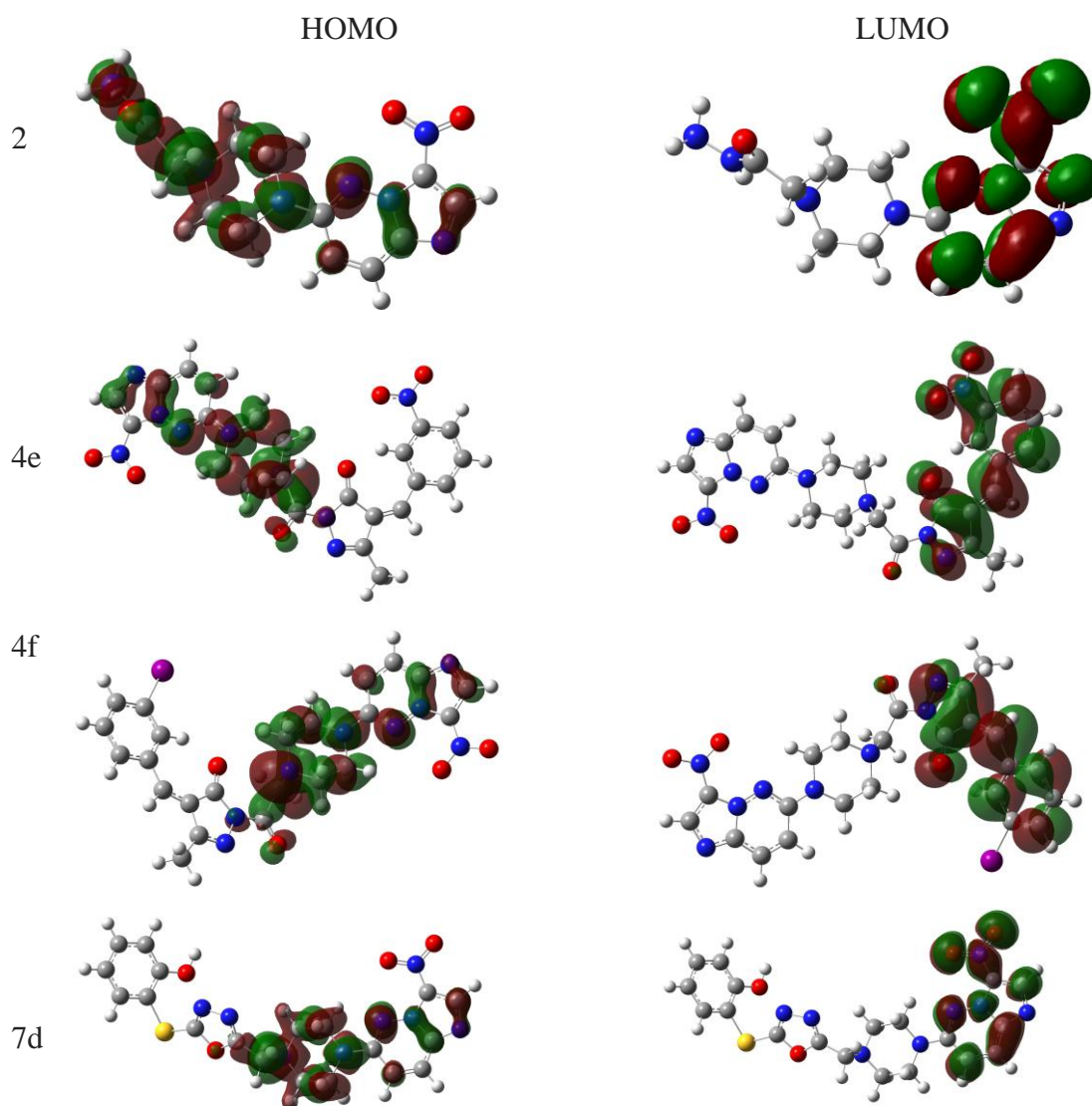


Fig. 3: HOMO and LUMO FMO of 2, 4e, 4f and 7d

Molecular docking studies of hydrazones and 1,3,4-oxadiazole derivatives onto BAX protein

Molecular docking is an important *in silico* technique, which predicts the mode of interaction between a small ligand and target protein for an established binding site. Binding energy informs us on the strength and how much affinity a compound binds to the pocket of a target protein (as shown in Fig. 4). A compound with a lower binding energy is preferred as a possible drug candidate and vice versa. Auto Dock Vina uses a sophisticated gradient optimization method in its local optimization procedure. Table- 2 shows the binding affinity of the eighty synthesized compounds as simulated by Auto Dock Vina ranging from -6.4 to -7.4. However, compounds **4f**, **4e** showed a stronger binding affinity compared with rest compounds. Despite hydrogen, Van der Waal, and pi bonds stabilizing interactions between the ligands and amino acid residues present in the active site of the protein, a strong hydrogen bond is present in the interaction between ligands and receptor that has been shown in the binding pockets (Fig.4). **RG37;GLY39;GLN32;MET38;THR14;GLN18;THR22; SER55; GLY157;ARG134;TRP139;ARG89;ASN104;PHE105;ASP102;ASP53;VAL50;THR22;TRP158;GLY157;ASP53; TRP139;ASP142;** are the amino acid residues in the binding pockets of BAX that are responsible for the various interactions between these proteins and the various ligands docked.

The relative abundance of the **ARG37;ARG89;GLN39;GLY157;MET38** amino acids present in the BAX proteins allows the compound of interest to bind with the active site for the inhibitory activity of the BAX proteins during the process of apoptosis.

The results of *in silico* molecular docking studies of compounds 6-7a with BAX protein are presented in Table- 3. It is observed that compound 7d showed greater binding affinity (-7.10 kcal/mol) with target receptor. The rest compounds (6, 7a, 7b, 7c, 7e, 7f) of the same series showed a good binding affinity (-6.2, to -6.9 kcal/mol). The studies reveal that majority of the compounds studied interacted with the amino acids, **ARG37;GLY39;GLN32;MET38** (polar and nonpolar); based on the nature of observed polarity, the compound of interest bind with the binding pocket that is polar in nature.

The relative abundance of the **ARG37;ARG89;GLN39;GLY157;MET38; ARG37;GLY39;GLN32;MET38** amino acids present in the BAX proteins allows the compound of interest to bind with the active site for the inhibitory activity of the BAX proteins during the process of apoptosis.

Several amino acid residues present in the binding pocket of proteins are involved in various interactions that occur between ligand and their targets. These residues are ligand dependent as the compound studied binds to different residues within the binding pocket. This amino acid residue is somewhat amphipathic with a long hydrophobic carbon tail close to the backbone and a positively charged amino group on the side chain. It is frequently found in the binding sites of proteins where they form hydrogen bonds with ligands and function in acid-base catalysis, making it a viable drug target.

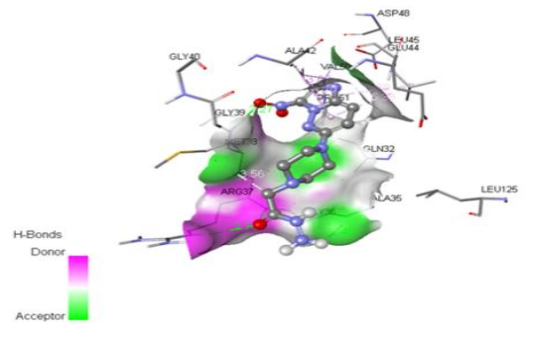
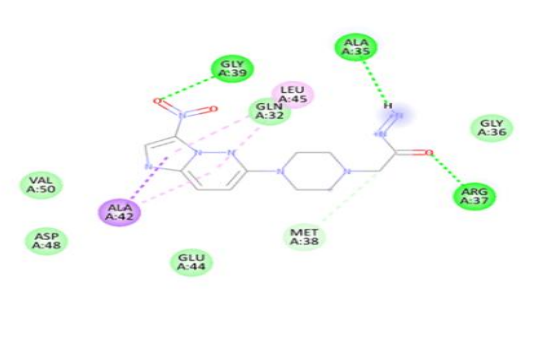
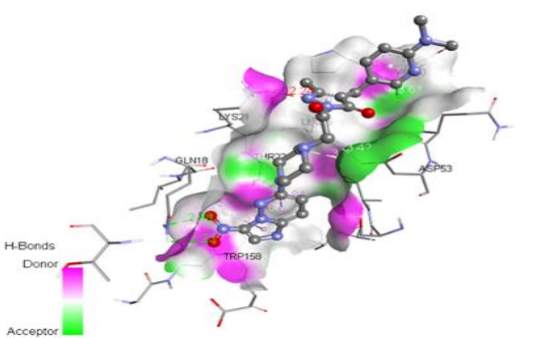
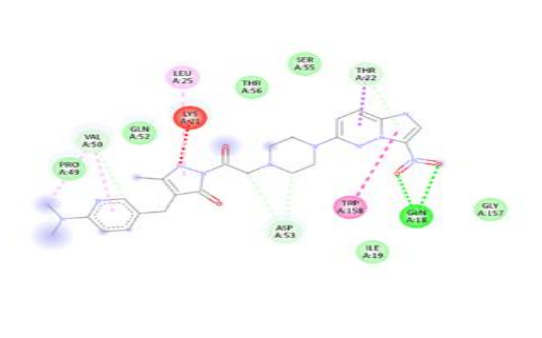
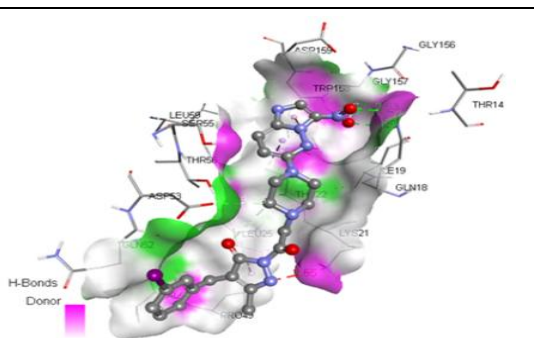
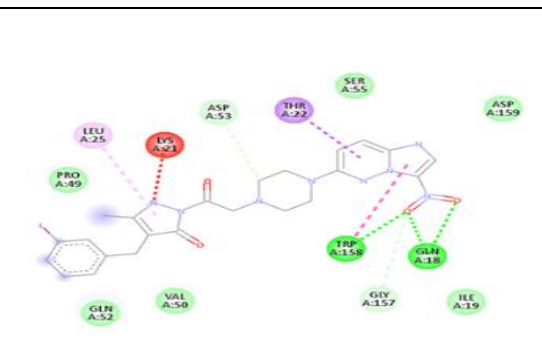
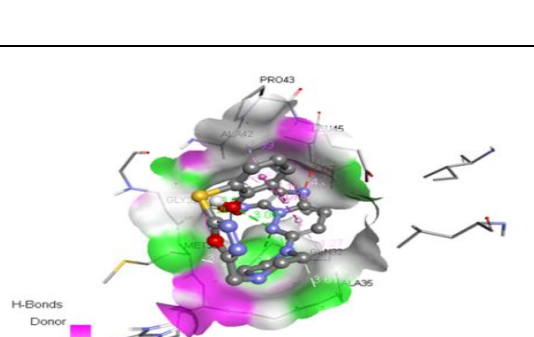
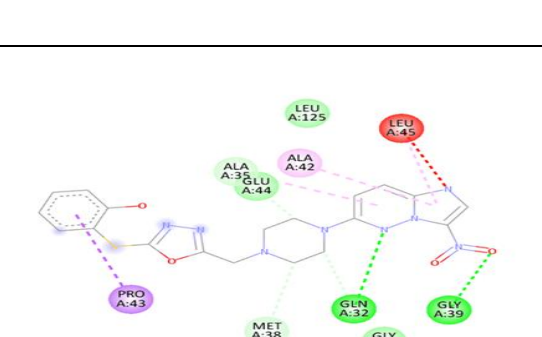
	3D	2D
2		
4e		
4f		
7d		

Fig. 4: 3D protein - ligand interactions with respect to bond distance ($\leq 4.0\text{\AA}$) and amino acids interactions (Pocket color representation shows the acceptor and donor forms of binding region). 2D protein - ligand interactions with respect to bond distance and amino acids interactions (Pocket color representation shows the acceptor and donor forms of binding region).

Table -2 The binding energy and interacting amino acid residues, respectively.

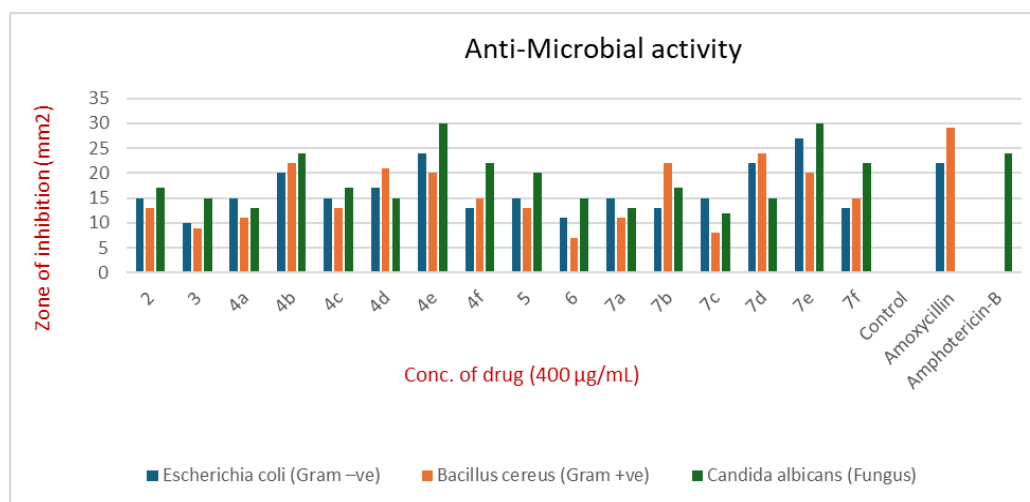
Protein Name	Protein PDB id	Compound	Binding Affinity (Kcal/mo)	RMSD lower bound (\AA)	RMSD upper bound (\AA)	Active amino acids
BAX	1F16	2	-6.6	2.888	3.519	ARG37;GLY39; ALA35;MET38;
		3	-7.1	2.995	3.272	ARG37;GLY39; GLN32;MET38;
		4a	-7.0	2.061	3.548	THR14;GLN18; THR22;SER55; GLY157;
		4b	-7.1	3.120	3.734	ARG134;TRP13 9;ARG89;
		4c	-7.0	1.991	2.272	ASN104;PHE10 5;ASP102;
		4d	-7.2	3.863	3.827	ARG37;GLY39; MET38
		4e	-7.3	1.171	3.708	GLN18;ASP53; VAL50;THR22;
		4f	-7.4	2.681	3.976	GLN18;TRP158; GLY157;ASP53;
	5	-6.4	2.340	3.136	ARG89;TRP139; ASP142;	

Table -3 The binding energy and interacting amino acid residues, respectively.

Protein Name	Protein PDB id	Compound	Binding Affinity (Kcal/mo)	RMSD lower bound (\AA)	RMSD upper bound (\AA)	Active amino acids
BAX	1F16	6	-6.2	1.742	2.261	ARG37;GLY39; GLN32;ALA35;
		7a	-6.8	2.834	3.447	ARG37;MET38;GLY 39;LEU45; ALA35;
		7b	-6.8	1.779	2.318	ARG37;MET38; GLY39;GLN32;
		7c	-6.8	1.800	2.370	LYS21;VAL50;TRP1 58;ASP159;THR22;
		7d	-7.0	3.186	3.672	GLY39;GLN32; GLU44;MET38;
		7e	-6.7	2.369	2.720	LYS21;TRP158;ASP 159;VLA50;THR22;
		7f	-6.9	3.861	3.826	SER55;THR54;SER1

Antimicrobial activity of substituted pyrazoles and 1,3,4-oxadiazole derivatives

From the results presented in graph-1 it is observed that some of the compounds showed excellent activity, while some show moderate to good activity. It is interesting to note that some compounds show less activity. Compounds **4e**, **4b** and **4d** showed excellent activity against all the bacterial strains while compounds **4a**, **4c**, **4f** & **5** showed good activities. Compound **3** displayed a weak activity.



Graph-1 Antimicrobial test results of 4-(substituted benzylidene)-3-methyl-1-(2-(4-(3-nitroimidazo[1,2-*b*]pyridazin-6-yl)piperazin-1-yl)acetyl)-1*H*-pyrazol-5(4*H*)-ones (**4a-f**) and 1-(3,5-dimethyl-1*H*-pyrazol-1-yl)-2-(4-(3-nitroimidazo[1,2-*b*]pyridazin-6-yl)piperazin-1-yl)ethanone (**5**). Antimicrobial test results of 3-nitro-6-(4-((5-(substituted-ylthio)-1,3,4-oxadiazol-2-yl) methyl) piperazin-yl) imidazo[1,2-*b*] pyridazines (**7a-f**).

All the tested compounds showed a significant antifungal activity with **4e** being more potent than the standard Amphotericin-B. Compounds **4b** and **4f** showed a good potency and the rest of the compounds showed less to moderate activity to *Candida albicans* (Fungus). Furthermore, it was observed that compound **4e** exhibits more potency against all tested organisms.

The results presented in Table-5 show that compounds **7d** and **7e** showed excellent activity against all the bacterial strains while compounds **7a**, **7b**, **7c** and **7f** showed good activity. Compound **6** displayed weak to moderate activity.

All the tested compounds showed a significant antifungal activity with **7e** & **7f** being more potent than the standard Amphotericin-B. Compounds **6**, **7b** & **7d** showed a good activity and compound **7c** shows less activity to *Candida albicans* (Fungus). Furthermore, it was observed that compound **7e** exhibits more potency against all tested organisms.

Thus, further structural modification of this scaffold may lead to a promising antibacterial and antifungal pharmacophore.

CONCLUSION:

The newly designed pyrazoles and 1,3,4-oxadiazole compounds have good synthetic accessibility, which indicates that these recently developed compounds can be effectively synthesized in the laboratory. To verify the stability of the molecules, DFT studies were completed by optimizing the structure and calculating the HOMO-LUMO gap. Of all the compounds examined, compound **2** had the largest band gap, implying more stability than the

other. BAX protein interactions were done, and the residues responsible for binding to the inhibitors of 1,3,4-oxadiazole substrates with high binding affinity were identified. Most of the compounds tested exhibit moderate to good antimicrobial activities. Based on the results obtained, we conclude that these 1,3,4-oxadiazole derivatives could be potential anti-cancer lead molecules for modulating the expression of BAX protein and supporting experimental testing.

ACKNOWLEDGEMENT:

All the authors are thankful to Department of Chemistry Sri Krishnadevaraya University, Ananthapuramu, India for their support and encouragement.

REFERENCES:

- I. Frieri M.; Kumar K.; Boutin A.; Antibiotic resistance. *J. Infect Public Health*. 2017, 10, 369.
- II. Aslam B.; Wang W.; Arshad M.I.; Khurshid M.; Muzammil S.; Rasool M. H; et al. Antibiotic resistance: a rundown of a global crisis. *Infect Drug Resist*. 2018, 11, 1645.
- III. Årdal C.; Balasegaram M.; Laxminarayan R.; McAdams D.; Outtersson K.; Rex J. H.; et al. Antibiotic development economic, regulatory and societal challenges. *Nat Rev Microbiol*. 2019, 18, 267.
- IV. Lomazzi M.; Moore M.; Johnson A.; Balasegaram M.; Borisch B.; Antimicrobial resistance moving forward *BMC Public Health*. 2019, 19, 858.
- V. Laws M.; Shaaban A.; Rahman K.M.; Antibiotic resistance breakers: current approaches and future directions. *FEMS Microbiol Rev*. 2019, 43, 490.
- VI. Richardson L.A.; Understanding and overcoming antibiotic resistance. *PLOS Biol*. 2017, 15.
- VII. Mannam M.R.S.S.; Kumar P.; Chamarthi N.R.K.R.S.P.; Synthesis of novel 3-[(2R*)-2-[(2S*)-6-fluoro-3,4-dihydro-2H-chromen-2-yl]-2-hydroxyethyl]-urea/thiourea derivatives and evaluation of their antimicrobial activities. *Phosphorus, Sulfur, Silicon Relat Elements*. 2019, 195, 65.
- VIII. Naresh V.S.S.P.; Somarothu P.; Synthesis and antimicrobial activity of some novel fused heterocyclic moieties. *Organic. Communications*. 2013, 6, 78.
- IX. Mannam M.R.; Devineni S.R.; Pavuluri C.M.; Chamarthi N.R.; Kottapalli R.S.P.; Urea and thiourea derivatives of 3-(trifluoromethyl)- 5,6,7,8-tetrahydro-[1, 2, 4]triazolo[4,3-a]pyrazine: synthesis, characterization, antimicrobial activity and docking studies. *Phosphorus, Sulfur, Silicon Relat Elements*. 2019, 194, 922.
- X. Mannam M.R.S.S.; Kumar P.K.R.S.P.; Synthesis of novel 1-(5- (Benzylsulfinyl)-3-methyl-1,3,4-thiadiazol-2(3 H)-ylidene)- thiourea/urea derivatives and evaluation of their antimicrobial activities. *J Heterocycl Chem*. 2019, 56, 2179.
- XI. Maddali N.K.; Viswanath I.V.K.; Murthy Y.L.N.; Bera R.; Takhi M.; Rao N.S.; et al. Design, synthesis and molecular docking studies of quinazolin-4-ones linked to 1,2,3-triazol hybrids as *Mycobacterium tuberculosis* H37Rv inhibitors besides antimicrobial activity. *Med Chem Res*. 2019, 28, 559.
- XII. MA A.; A review: biological importance of heterocyclic compounds. *Der Pharma Chem*. 2017, 9, 141.
- XIII. Depa N.; Erothu H.; One-pot three-component synthesis of 3- aminoalkyl indoles catalyzed by molecular iodine. *ChemistrySelect*. 2019, 4, 9722.
- XIV. Ansari A.; Ali A.; Asif M.; Shamsuzzaman S.; Review: biologically active pyrazole derivatives. *N. J. Chem*. 2017, 41, 16.

- XV. Hassan A.S.; Askar A.A.; Naglah A.M.; Almehezia A.A.; Ragab A.; Discovery of new schiff bases tethered pyrazole moiety: design, synthesis, biological evaluation, and molecular docking study as dual targeting DHFR/DNA gyrase inhibitors with immunomodulatory activity. *Molecules*. 2020, 25, 2593.
- XVI. Cunha F.; Nogueira J.; de Aguiar A.; Synthesis and antibacterial evaluation of 3,5-Diaryl-1,2,4-oxadiazole derivatives. *J. Braz Chem. Soc.* 2018, 29, 2405.
- VII. Biernacki K.; Daško M.; Ciupak O.; Kubiński K.; Rachon J.; Demkowicz S.; Novel 1,2,4-oxadiazole derivatives in drug discovery. *Pharmaceuticals*. 2020, 13, 111.
- VIII. Parikh P.H.; Timaniya J.B.; Patel M.J.; Patel K.P.; Design, synthesis, and characterization of novel substituted 1,2,4-oxadiazole and their biological broadcast. *Med Chem Res*. 2020, 29, 538.
- IX. Dasari S.R.; Tondepu S.; Vadali L.R.; Seelam N.; PEG-400 mediated an efficient eco-friendly synthesis of new isoxazolyl pyrido[2,3-d] pyrimidines and their anti-inflammatory and analgesic activity. *Synth Commun*. 2020, 50, 2950.
- XX. Perla P.; Seelam N.; Bera R.; Design and synthesis of novel 1a,3,4- oxadiazole derivatives as cytotoxic agents: a combined experimental and docking study. *Russ J Org Chem*. 2020, 56, 924.
- XI. Alam O.; Naim M.; Nawaz F.; Alam M.J.; Alam P.; Current status of pyrazole and its biological activities. *J. Pharmacy Bioallied Sci.* 2016, 8, 2.
- XII. El Shehry M.F.; Abbas S.Y.; Farrag A.M.; Fouad S.A.; Ammar Y.A.; Synthesis and biological evaluation of 3-(2,4-dichlorophenoxyethyl)-1-phenyl-1H-pyrazole derivatives as potential antitumor agents. *J. Iran Chem. Soc.* 2020, 17, 2567.
- XIII. Liu H.; Yang G.S.; Liu C.B.; Lin Y.; Yang Y.; Gong Y.N.; Syntheses, crystal structures, and antibacterial activities of helical M(II) phenyl substituted pyrazole carboxylate complexes. *J. Coord Chem*. 2014, 67, 572.
- XIV. Hassan S.; Synthesis, antibacterial and antifungal activity of some new pyrazoline and pyrazole derivatives. *Molecules*. 2013, 18, 2683.
- XV. Dasari S.R.; Tondepu S.; Vadali L.R.; Seelam N.; Design, synthesis and molecular docking studies of novel pyrazole benzimidazole derivatives as potent antibacterial agents. *Asian J Chem*. 2019, 31, 2733.
- XVI. Koteswara Rao C.P.; Rao T.B.; Charan G.K.; Srinu B.; Maturi S.R.; Synthesis and anticancer evaluation of 2-{4-[5-(5-substituted arylpyrimidin-2-yl)-1H-pyrazol-3-yl]-phenyl}thiazolo[4,5-b]pyridine derivatives. *Russ J. Gen Chem*. 2019, 89, 1023.
- VII. Karrouchi K.; Radi S.; Ramli Y.; Taoufik J.; Mabkhot Y.; Al-aizari F.; et al. Synthesis and pharmacological activities of pyrazole derivatives: a review. *Molecules*. 2018, 23, 134.
- VIII. Kumar D.; Patel G.; Chavers A.K.; Chang K.H.; Shah K.; Synthesis of novel 1,2,4-oxadiazoles and analogues as potential anticancer agents. *Eur J Med Chem*. 2011, 46, 3085.
- IX. Caneschi W.; Enes K.B.; Carvalho de Mendonça C, de Souza Fernandes F, Miguel FB, da Silva Martins J, et al. Synthesis and anticancer evaluation of new lipophilic 1,2,4 and 1,3,4-oxadiazoles. *Eur J Med Chem*. 2019, 165, 18.
- XX. Suhail H.D.; Mazin N.M.; Ekhlhas Qanber J.; Rawaa M.O.H.; Synthesis, characterization and antibacterial evaluation of 1,3,4-oxadiazole derivatives. *Int. J. Res. Pharm. Sci.* 2019, 10, 2342.
- XI. Neeraja P, Srinivas S, Mukkanti K, Dubey PK, Pal S. 1H-1,2,3- Triazolyl-

substituted 1,3,4-oxadiazole derivatives containing structural features of ibuprofen/naproxen: their synthesis and antibacterial evaluation. *Bioorganic Med Chem Lett.* 2016, 26, 5212.

- XII. Titi A.; Messali M.; Alqurashy B.A.; Touzani R.; Shiga T.; Oshio H.; et al. Synthesis, characterization, X-Ray crystal study and bioactivities of pyrazole derivatives: Identification of antitumor, antifungal and antibacterial pharmacophore sites. *J Mol Struct.* 2020, 1205, 127625.
- XIII. Anand Mohan J.; Md. Mansoor A.; Design, synthesis and antibacterial evaluation of hybrid curcumin based pyrazole derivatives. *Int J pharma Bio Sci.* 2020, 10, 94.
- XIV. Baral N.; Mohapatra S.; Raiguru B.P.; Mishra N.P.; Panda P.; Nayak S.; et al. Microwave-assisted rapid and efficient synthesis of new series of chromene-based 1,2,4-oxadiazole derivatives and evaluation of antibacterial activity with molecular docking investigation. *J Heterocycl Chem.* 2019, 56, 552.
- XV. Shetnev A.; Baykov S.; Kalinin S.; Belova A.; Sharoyko V.; Rozhkov A.; et al. 1,2,4-Oxadiazole/2-imidazoline hybrids: multi-target directed compounds for the treatment of infectious diseases and cancer. *Int. J. Mol. Sci.* 2019, 20, 1699.
- XVI. Poater J.; Duran, M.; Solà, M.; Silvi, B. Theoretical Evaluation of Electron Delocalization in Aromatic Molecules by Means of Atoms in Molecules (AIM) and Electron Localization Function (ELF) Topological Approaches. *Chem. Rev.* 2005, 105, 3911.
- XVII. Morris R.; Huey W.; Lindstrom M. Sanner.; Belew R.; Goodsell D.S.; Olson A.; J, *J. Comput. Chem.*, **2009**, 30.
- XVIII. Chinthakunta, N.; Cheemanapalli, S.; Chinthakunta S.; Anuradha C.; Chitta S. K.; A new insight into identification of in silico analysis of natural compounds targeting GPR120, *Netw. Model. Anal. Health Inform. Bioinform.*, 2018, 7, 1.
- XIX. Ahsan M.J.; 1, 3, 4-Oxadiazole Containing Compounds as Therapeutic Targets for Cancer Therapy, *Mini Rev. Med. Chem.*, 2021.
- XL. Subbarao B.; Sanjeeva P.; Karuna Raman P.; Satyanarayana Swamy V.; Kamala Prasad V. Venkata Ramana P.; "Asian Journal of Organic & Medicinal Chemistry." 2022, 7, 187.
- XLI. Goodsell D.S.; Morris G.M.; Olson A.J.; Automated docking of flexible ligands: Applications of autodock. *J. Mol. Recognit.* 1996, 9, 1.
- LII. Kaiser S.; Smidt S.P.; Pfaltz, A.; Iridium Catalysts with Bicyclic Pyridine Phosphinite Ligands: Asymmetric Hydrogenation of Olefins and Furan Derivatives. *Angew. Chem. Int. Ed.* 2006, 45, 5194.

Received on November 25, 2024.